Appendix Table of Contents:

Appendix Figure S1

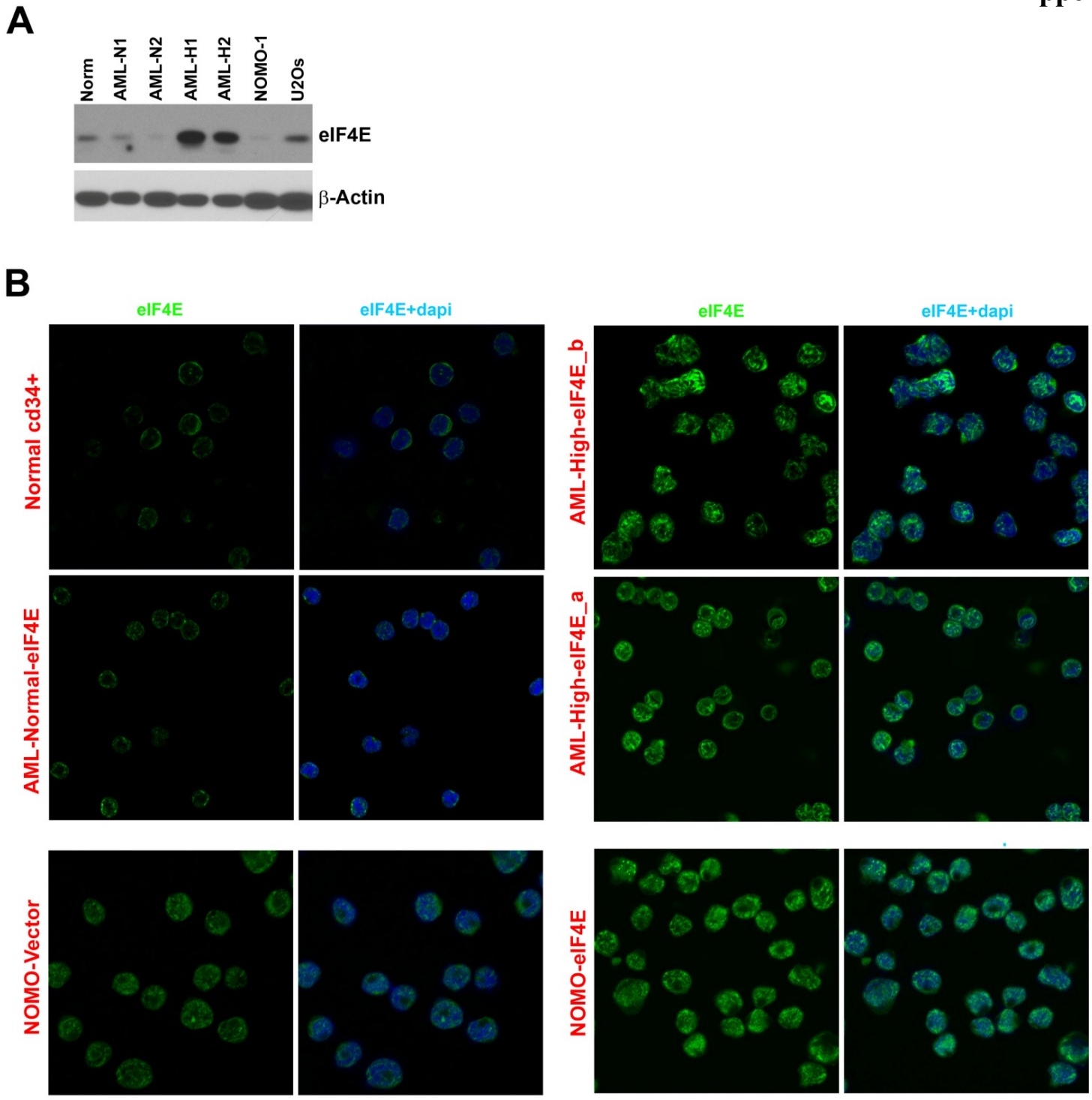

Appendix Figure S1

C

>NOMO1SF3B1_SF3B1Fw5

NNNNNNNNNGNTGCTGGTCTGGCTACTATGATCTCTACCNTGAGACCTGATATAGATAACATGGATGAGTA
TGTCCGTAACACAACAGCTAGAGCTTTTGCTGTTGTAGCCTCTGCCCTGGGCATTCCTTCTTTATTGCCCTTC
TTAAAAGCTGTGTGCAAAAGCAAGAAGTCCTGGCAAGCGAGACACACTGGTATTAAGATTGTACAACAGA
TAGCTATTCTTATGGGCTGTGCCATCTTGCCACATCTTAGAAGTTTAGTTGAAATCATTGAACATGGTCTTGT
GGATGAGCAGCAGAAAGTTNNGACCATCAGTGCTTTGGCCATTGCTGCCTTGGCTGAAGCAGCAACTCCT
TATGGTATCGAATCTTTTGATTCTGTGTTAAAGCCTTTATGGAAGGGTATCCGCCA

Equal mix of A and C (CGG=wt)

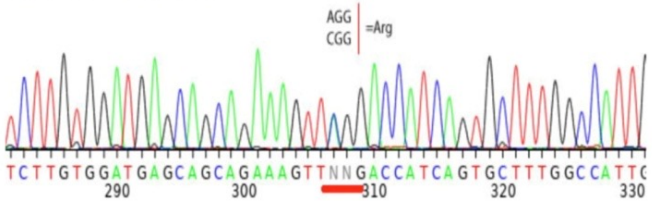

>NOMO1SF3B1_SF3B1Fw1

NNNNNNNNNNCTGNGTGCAANGCAAGAAGTCCTGGCAAGCGAGACACACTGGTATTAAGA
TTGTACAACAGATAGCTATTCTTATGGGCTGTGCCATCTTGCCACATCTTAGAAGTTTAG
TTGAAATCATTGAACATGGTCTTGTGGATGAGCAGCAGAAAGTTNGGACCATCAGTGCTT
TGGCCATTGCTGCCTTGGCTGAAGCAGCAACTCCTTATGGTATCGAATCTTTTGATTCTG
TGTTAAAGCCTTTATGGAAGGGTATCCGCCA

Equal mix of A and C (CGG=wt)

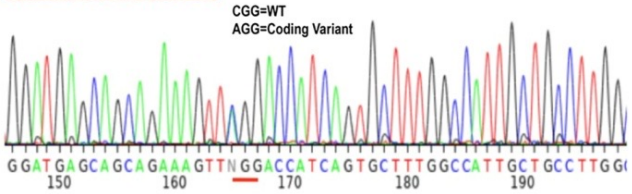

rs16865307

chr2:197402104 (GRCh38.p12); Gene ConsequenceSF3B1 : Missense Variant

Alleles:G>A / G>T

Molecule type	Change	Amino acid[Codon]	SO Term
SF3B1 transcript variant 1	NM_012433.4:c.2104C>T	R [CGG] > W [TGG]	Coding Sequence Variant
SF3B1 transcript variant 1	NM_012433.4:c.2104C>A	R [CGG] > R [AGG]	Coding Sequence Variant
SF3B1 transcript variant 2	NM_001005526.2:c.	N/A	Genic Downstream Transcript Variant
SF3B1 transcript variant 3	NM_001308824.1:c.	N/A	Genic Downstream Transcript Variant
SF3B1 transcript variant X1	XR_001738680.2:n.2149C>T	N/A	Non Coding Transcript Variant
SF3B1 transcript variant X1	XR_001738680.2:n.2149C>A	N/A	Non Coding Transcript Variant
SF3B1 transcript variant X2	XR_001738681.1:n.	N/A	Genic Downstream Transcript Variant
SF3B1 transcript variant X3	XR_241302.2:n.	N/A	Genic Downstream Transcript Variant
splicing factor 3B subunit 1 isoform 1	NP_036565.2:p.Arg702Trp	R (Arg) > W (Trp)	Missense Variant
splicing factor 3B subunit 1 isoform 1	NP_036565.2:p.Arg702=	R (Arg) > R (Arg)	Synonymous Variant

NOMO1-SRSF2_SRSFFw1

TATGGNTGCCNTGGACGGGGCCGTGCTGGACGGCCGCGAGCTGCGGGTGCAAATGGCGCGCTACGGCCGCCCCCGGACTCACACCACA
GCCGCCGGGGACCGCCACCCCGCAGGTACGGGGGCGGTGGCTACGGACGCCGGAGCCGCAGCCCTAGGCGGCGTCGCCGCAGCCGATCC
CGGAGTCGGAGCCGTTCCAGGTCTCGCAGCA

Corresponds to WT

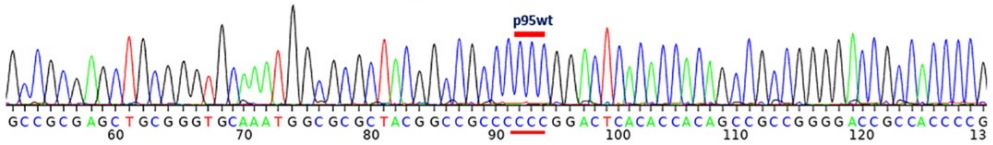

NOMO1-U2AF35_U2AF35Fw4

AAAGTCAACTGTTCATTTTATTTCAAAATTGGAGCATGTCGTCATGGAGACAGGTGCTCTCGGTTGCACAATAAACCGACGTTTAGCCAGAC
CATTGNCCTCTTGAACATTTACCGTAACCCTCAAAACTCTTCCCAGACTGCTGACGGNTTGCNCTGTGCCGTGAGCGATGTGGAGATGCAG

Corresponds to WT

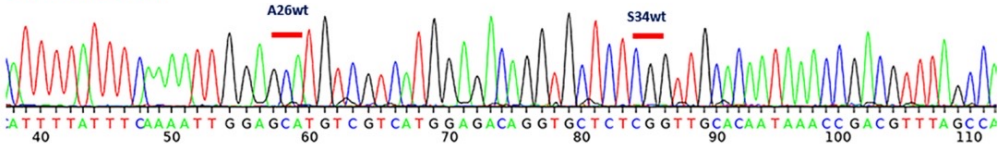

NOMO_4EU2AF35_u2af35Q157R1GCCGCAGCTCTCTGGAAATGGGCTTCAAATGCATGAAGTTGCAGAAGCCGCCTCGTGTGCATTC
TCCCATCTCATACTGACGGCAGCAGGCTTCTCTGAAGTCCGTCACGGGTGACAGCTCGGCGTGGATCGGCTGTCCATTAAACCAACGGTTA
TTCAAGTCAATCACAGCCTTTTCCGCATCTTCCTCACGGCGAAACTTGACGTACACGTTCCCCACCAGGTGGTCTCCCAGGTTGTCACAGA
CGTTCATCTCCTCTACTTCCCCATACTTCTCCTCCATTTCTGTAAAAACCTCCTCAAAAAACTCATCATAGTGTTCCTGCATCTCCACATCGCTC
ACGGCACAGCGCAAACCGTCAGCAGACTGGGAANAGNTTTGAGGGTTACGGTAAATGTTCAAGAGGGCAATGGTCTGGCTAAACGTCG
GTTTATTGTGCAACCGAGAGCACCTGTC TCCATGACGACATGCTCCAATTTTGAAATAAAATGAACAGNTGACTTTGTCTTTCTCGGT
GNCGAAGATGGANGNCANATACTCC

Corresponds to WT

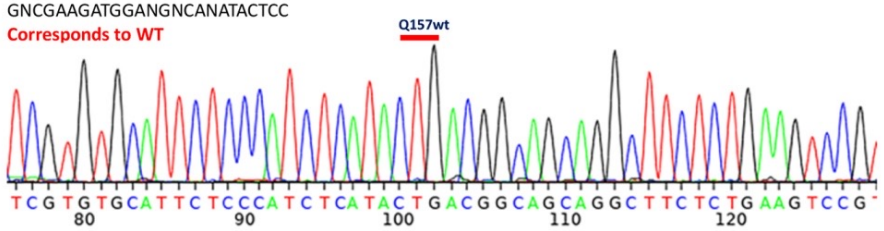

Appendix Figure S1. eIF4E localization and levels in various cells and sequence status of splicing factors showing WT phenotype. **A.** WB analysis of endogenous eIF4E levels in U2OS and NOMO-1 cell lines compared to primary AML samples with high (AML-H) and normal (AML-N) eIF4E levels, as well as bone marrow mononuclear cells from healthy volunteers (Norm). β-actin was used as a loading control. **B.** Localization of eIF4E in NOMO-1 Vector and eIF4E cells compared to primary AML specimens with high (AML-H) and normal (AML-N) eIF4E levels, as well as bone marrow mononuclear cells from healthy volunteers cd34+ cells (Norm). Confocal micrographs of cells stained with anti-eIF4E antibodies (in green) and DAPI (in blue) as a nuclear marker. Single (eIF4E) and overlaid (eIF4E+DAPI) channels are shown. Micrographs are single sections through the plane of the cells with 63x magnification. Confocal settings were identical for all samples and thus the differences in staining intensity are related to the levels of eIF4E; a and b represent two different patients. **C.** Sequencing of SF3B1, SRSF2 and U2AF1 genes for NOMO-1 cells showing WT phenotype. SF3B1 showed heterozygous status with allele variant already reported. This allele does not alter the amino acids in the protein produced *i.e.,* results in a silent mutation.

Appendix Figure S2

A

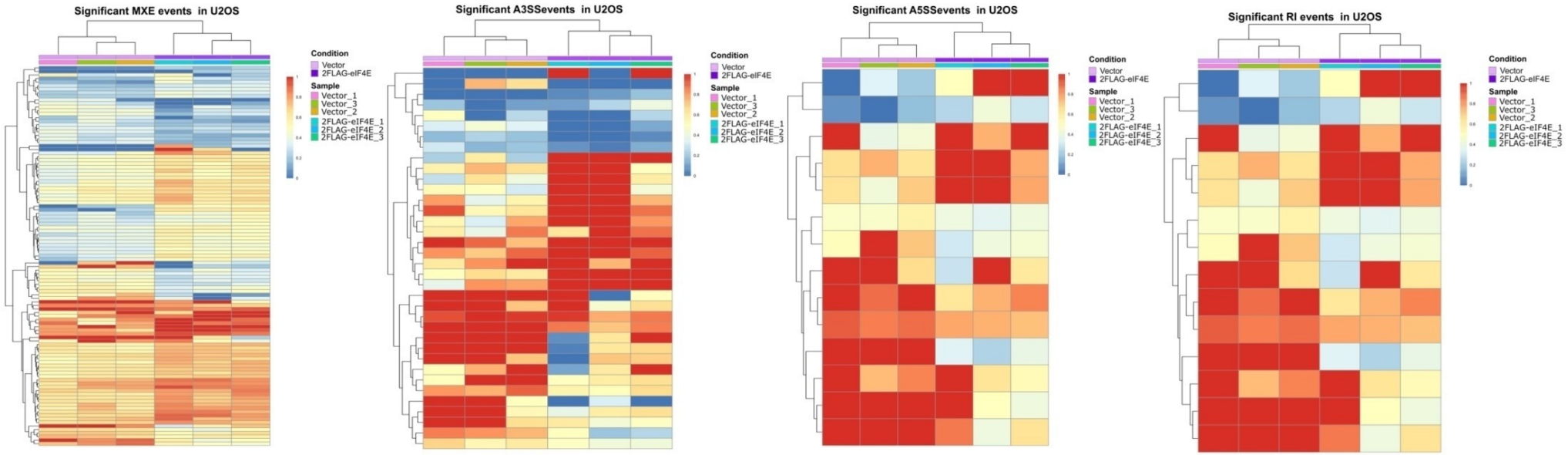

Appendix Figure S2

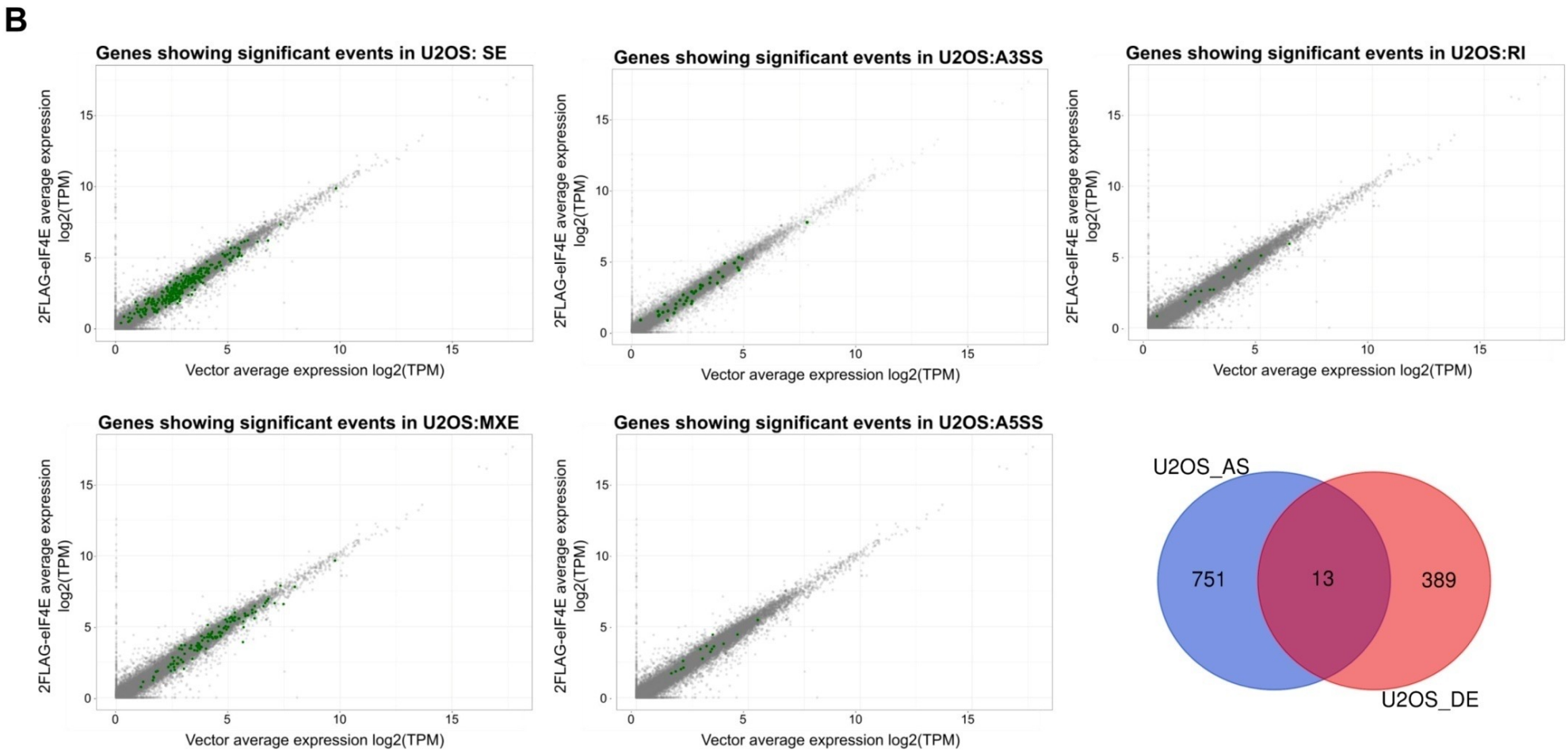

Appendix Figure S2. Alternative splicing reprogramming upon eIF4E overexpression is based solely on eIF4E levels and does not elicit changes to most AS target RNA levels. A. Unsupervised hierarchal clustering indicates that events segregate solely on eIF4E levels in U2OS cells. The resulting heatmaps of inclusion levels for indicated event type are shown. Events considered have an FDR-adjusted p-value <0.1 and an absolute inclusion value >0.1. SE events are shown in Fig 3C. **B.** Alternatively spliced targets are not characterized by differential RNA expression in 2FLAG-eIF4E versus Vector U2OS cells: Scatter plots show average $\log_2$(TPM) for each condition. Targets that have one or more splicing events are highlighted in green. Lower right panel. Venn diagram showing the overlap between differentially expressed genes (DE) and alternatively spliced targets (AS) is low, with only 13 targets in common.

Appendix Figure S3

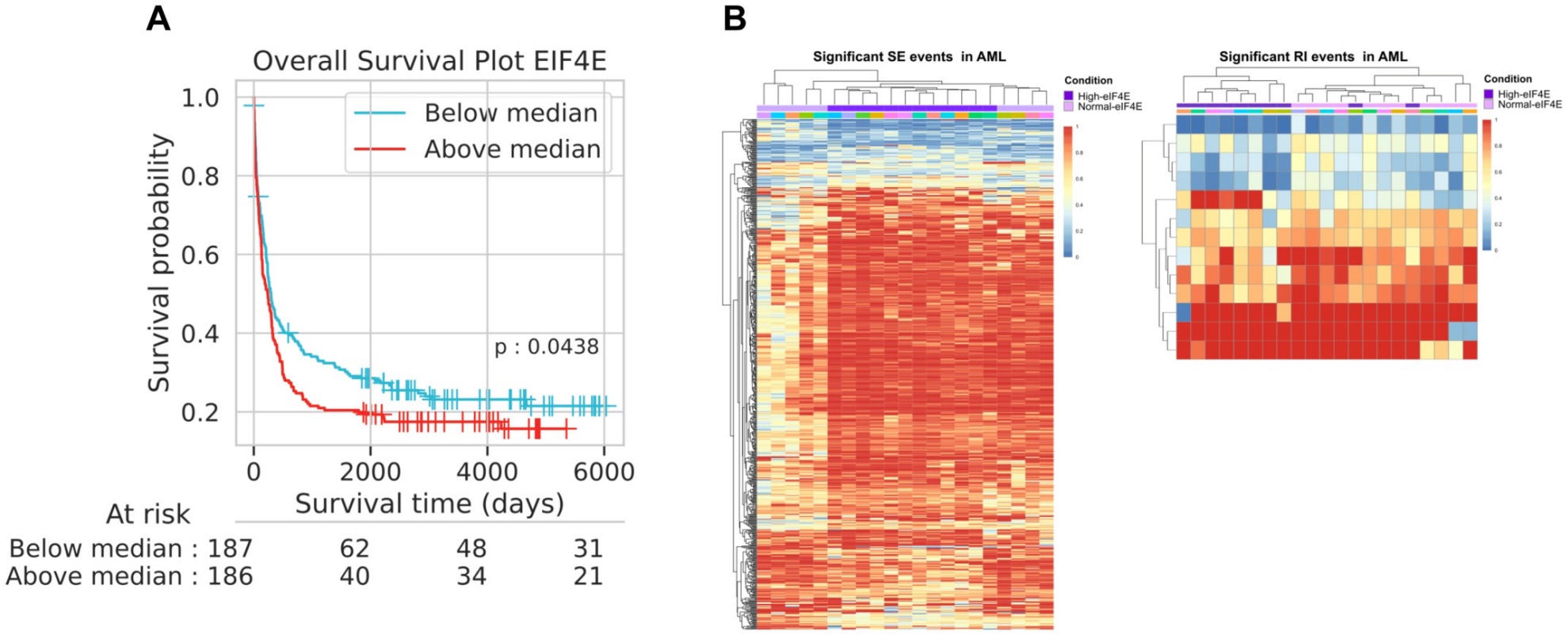

Appendix Figure S3

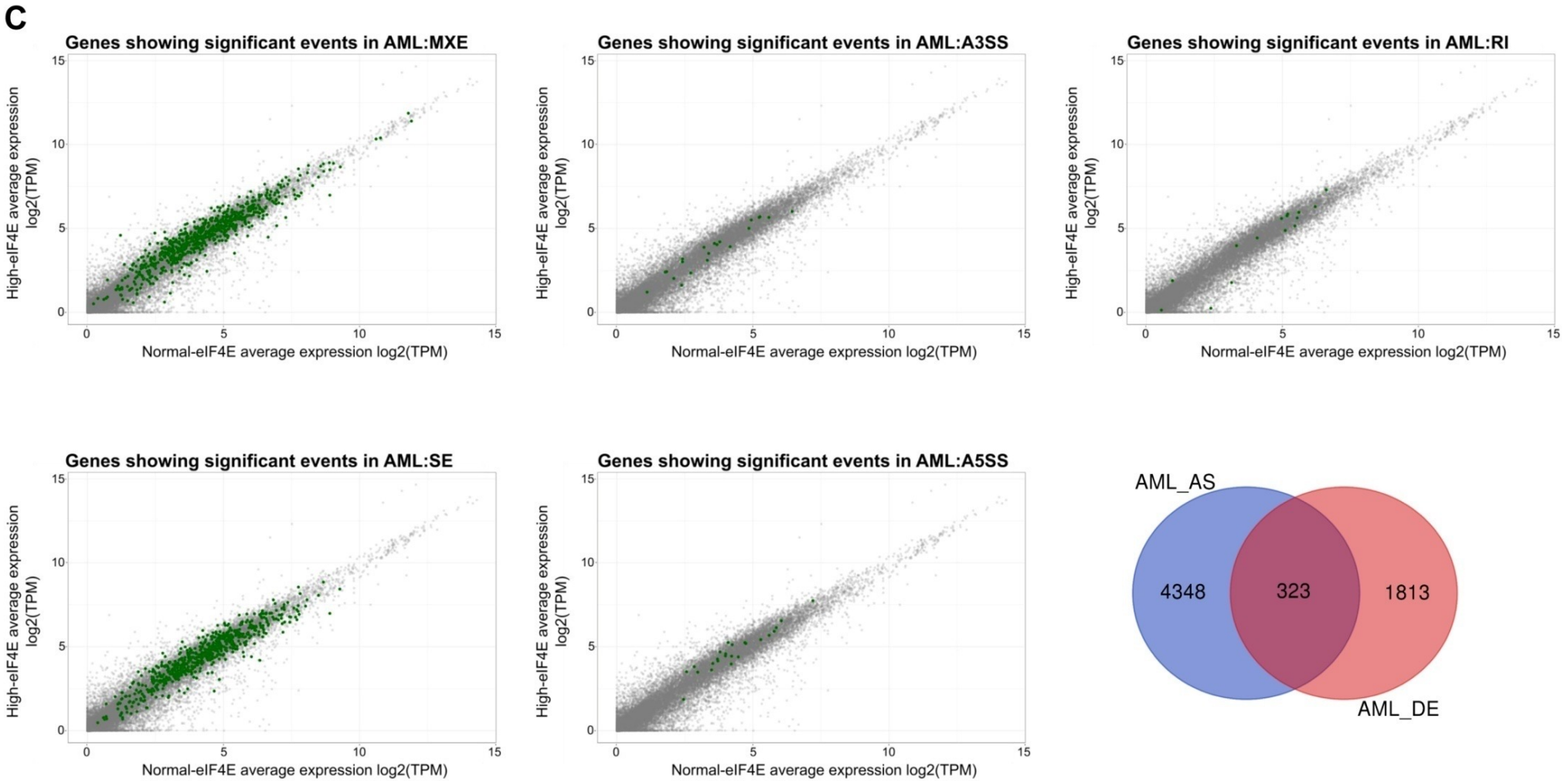

Appendix Figure S3. High-eIF4E levels are correlated with low survival in AML patients and alternative splicing. A. Survival analysis of the Leucegene cohort. The cohort was divided in two groups based on eIF4E expression levels (below the median, blue and above the median, orange). Log Rank test was performed and shows a significant difference in survival between the two groups (p-value<0.05).
B. Unsupervised hierarchal clustering of indicated AS events in primary AML specimens. The resulting heatmaps show that SE events segregate on eIF4E levels (High-eIF4E versus Normal-eIF4E specimens), whereas in RI events, clustering on eIF4E levels is evident but there are two outliers that behave more like Normal-eIF4E AML. Heatmaps of inclusion levels for SE and RI events are shown here and for MXE events in Figure 6E. Events considered have an FDR-adjusted p-value <0.1 and an absolute inclusion value >0.1. **C.** Alternatively spliced targets are not differentially expressed in High-eIF4E versus Normal-eIF4E AML patient' cells: Scatter plots showing average log2 (TPM) for each condition. Targets that have one or more splicing event(s) are highlighted in green. Venn diagram showing the overlap between differentially expressed genes (DE) and alternatively spliced targets (AS) is low, with only 7% overlap.

Appendix Figure S4

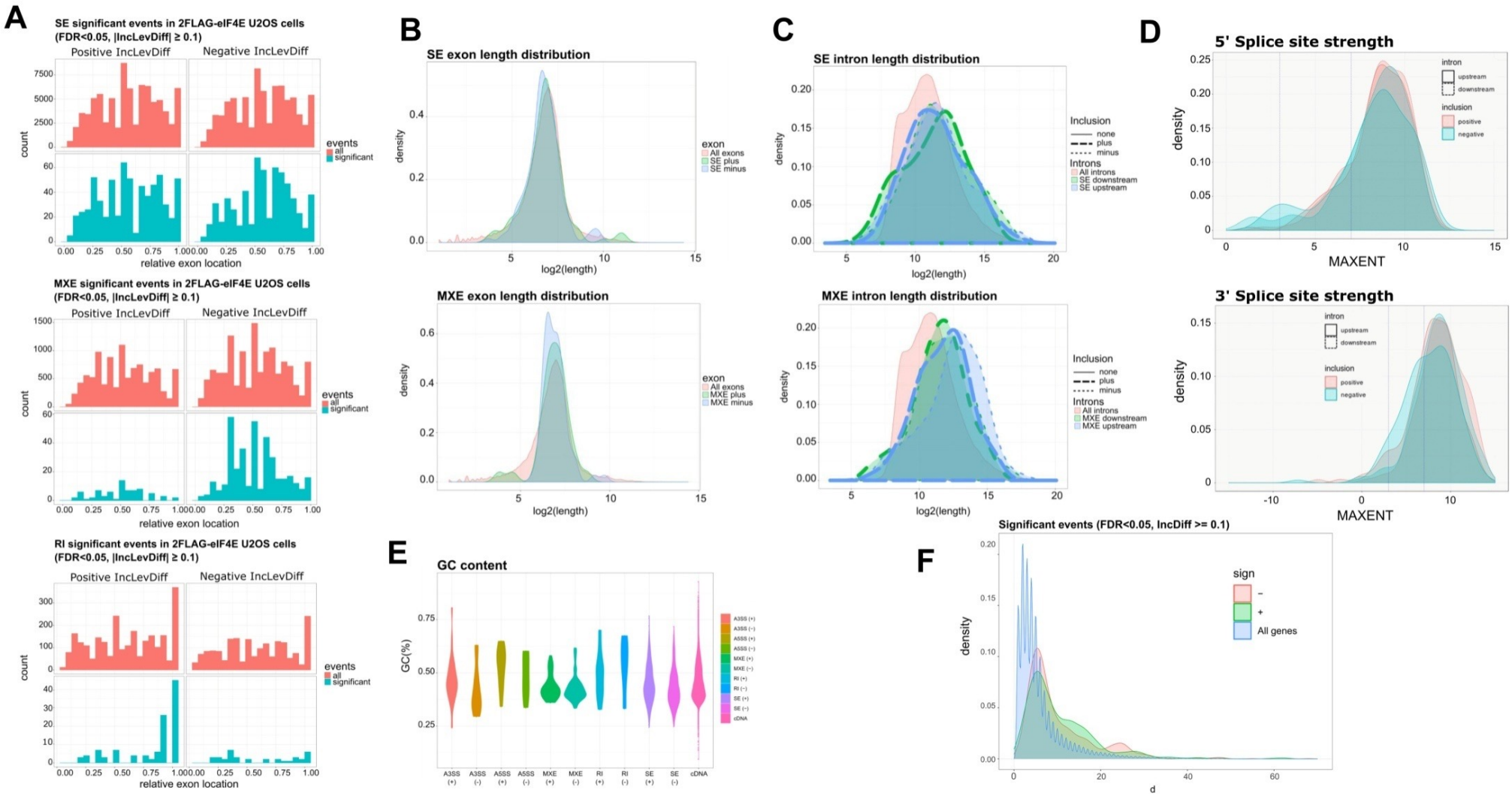

Appendix Figure S4. Characterization of eIF4E-dependent alternative splicing events in U2OS cells. A. Relative location of significant splicing events along the length of the transcripts with each transcript divided into equal fractions where 0.00 indicates the 5' end and 1.00 the 3' end. Events are shown for all transcripts (pink) and those that were significantly different between 2FLAG-eIF4E and Vector cells (cyan). To capture the most robust differences, FDR adjusted p-values<0.05 and absolute inclusion level differences >0.1 are shown, and data were segregated based on the sign of the inclusion levels differences "Positive IncLevDiff" and "Negative IncLevDiff". **B.** The length distribution of exons involved in alternate splicing events (FDR<0.1, absolute inclusion level difference > 0.1) compared to all exons. Plus refers to positive inclusion level differences (green), negative differences (blue) and for comparison, distribution of lengths for all exons (orange). **C.** The length distribution of introns involved in alternate splicing events (FDR<0.1, absolute inclusion level differences > 0.1) compared to length distribution for all introns (in orange). The intron is downstream (green) or upstream (blue) of the splicing event. Plus refers to positive inclusion level differences and minus refers to negative differences. **D.** Prediction of splice site strength based on sequence analysis around splice site events using MAXENT. Positive refers to positive inclusion level differences (orange), minus refers to negative inclusion level differences (blue). The position of the 5' splice site upstream (solid line) or downstream (dashed line) of the event is shown. **E.** Comparison of GC content in introns involved in significant events (FDR-adjusted p-value <0.1, absolute inclusion level difference > 0.1) compared with all cDNA. The GC content for cDNA was computed on all transcripts from Gencode version 32 of the human genome. "+" indicates positive inclusion level difference, and "–" a negative one. **F.** Analysis of the number of exons per targeted transcripts relative to the number of exons in all transcripts expressed. More exons were seen for both increased and decreased inclusions level differences (p<.001 using the Kolmogorov-Smirnov test) in high-eIF4E cells. "positive" refers to positive inclusion level differences (green), "negative" refers to negative differences (red) and all genes (blue).

Appendix Figure S5

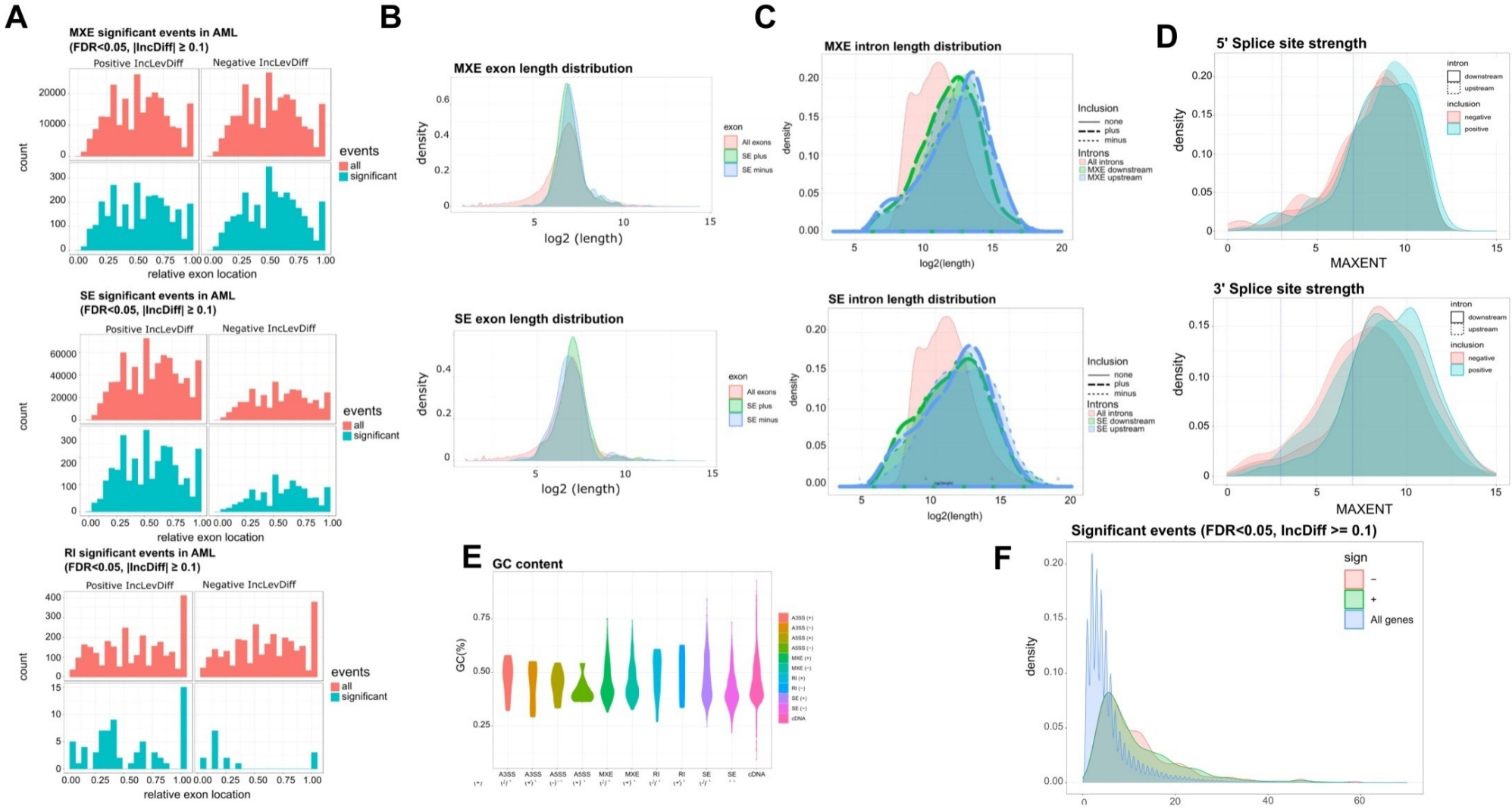

Appendix Figure S5. Characterization of eIF4E-dependent alternative splicing events in AML specimens. A. Relative location of significant splicing events along the length of the transcripts with each transcript divided into equal fractions where 0.00 indicates the 5' end and 1.00 the 3' end. Events are shown for all transcripts (pink) and those that were significantly different between High-eIF4E and Normal-eIF4E cells (cyan). To capture the most robust differences, FDR adjusted p-values<0.05 and absolute inclusion level differences >0.1 are shown, and data were segregated based on the sign of the inclusion levels differences "Positive IncLevDiff " and "Negative IncLevDiff ". **B.** The length distribution of exons involved in alternate splicing events (FDR<0.1, absolute inclusion level difference > 0.1) compared to all exons. **C.** The length distribution of introns involved in alternate splicing events (FDR-adjusted p-value<0.1, absolute inclusion level differences > 0.1) compared to length distribution for all introns (in orange). The intron is downstream (green) or upstream (blue) of the splicing event. Plus refers to positive inclusion level differences and minus refers to negative differences. **D.** Prediction of splice site strength based on sequence analysis around splice site events using MAXENT. "positive" refers to positive inclusion level differences (orange), "negative" refers to negative differences (blue). The position of the 5' splice site upstream (solid line) or downstream (dashed line) of the event is shown. **E.** Comparison of GC content in introns involved in significant events (FDR-adjusted p-value <0.1, absolute inclusion level difference > 0.1) compared with all cDNA. The GC content for cDNA was computed on all transcripts from Gencode version 32 of the human genome. "+" indicates positive inclusion level difference, and "–"a negative one. **F.** Analysis of the number of exons per targeted transcripts relative to the number of exons in all transcripts expressed. More exons were seen for both increased and decreased inclusions level differences (p<.001 using the Kolmogorov-Smirnov test) for High-eIF4E cells. "positive" refers to positive inclusion level differences (green), "negative" refers to negative differences (red) and all genes (blue).

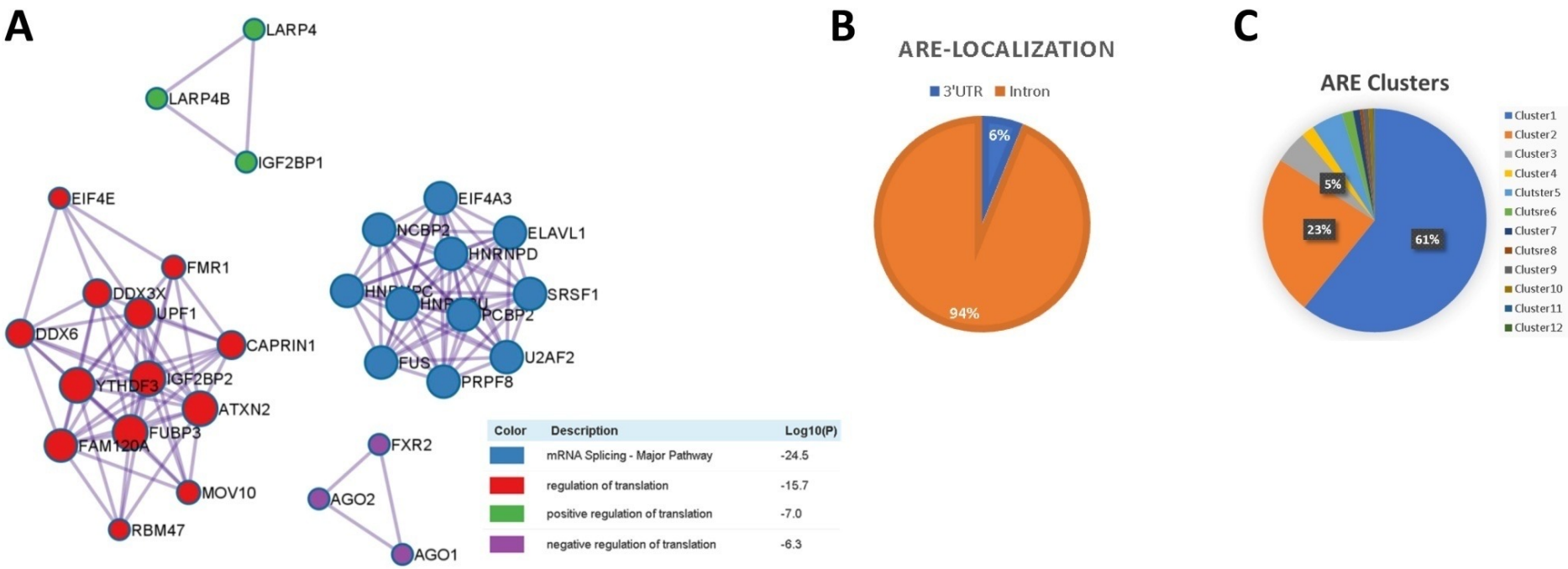

Appendix Figure S6. PRP8, U2AF2 and ARE-binding proteins were identified as potential regulators of eIF4E regulated AS target RNAs. A. MCODE networks identified from AURA analysis with 20% coverage of eIF4E-AS targets. Pathway and process enrichment analysis has been applied for each MCODE component and the best-scoring term by p-value is shown. **B.** Pie chart representing the proportion of ARE in eIF4E-AS targets based on their localization. Orange for intronic ARE and blue for ARE in 3'UTR. **C.** Pie chart showing the percentage of each ARE cluster type within eIF4E-AS targets.

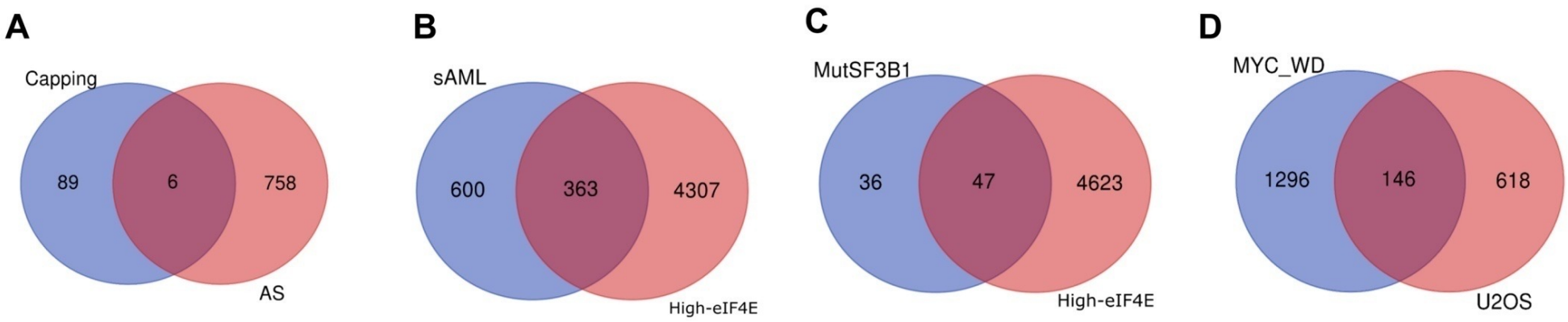

Appendix Figure S7. Comparisons of U2OS and AML related alternative splicing targets with published datasets. A. Venn diagram showing the overlap between eIF4E-Capping (Culjkovic-Kraljacic *et al*, 2020a) and eIF4E-AS targets identified here. **B.** Comparison of alternatively spliced targets in secondary AML (sAML; (Crews *et al*, 2016)) with AS transcripts in High-eIF4E AML patients' samples here. **C.** Venn diagram showing the overlap between alternatively spliced targets in AML samples harbouring SF3B1 mutations (MutSF3B1, mainly the hotspot mutation K700; (Hershberger *et al*, 2021) and AS targets in High-eIF4E AML patient's samples. **D.** Comparison of splicing targets following Myc withdrawal in Myc/myrAKT1 Prostate cancer cells (MYC-WD) with alternatively spliced targets upon eIF4E overexpression (Phillips *et al*, 2020).